Coseismic gravity changes of the 2010 earthquake in central Chile from satellite gravimetry

Kosuke Heki[1] and Koji Matsuo[1]

[1] The first map of coseismic changes in gravity and geoid height has been drawn using the data from the Gravity Recovery and Climate Experiment (GRACE) satellites for the 2004 Sumatra-Andaman earthquake. Here we present the second case of coseismic gravity change observation by satellite gravimetry, i.e., the change caused by an interplate thrust earthquake that occurred on 27 February, 2010 in Central Chile (M_w = 8.8). Gravity showed a negative jump with the largest drop of ~5 μgal on the back-arc side. The observed changes agree with those calculated assuming the realistic earth and fault parameters inferred from coseismic displacements of Global Positioning System (GPS) stations. Gravity in this area shows large seasonal and inter-annual variability, and postseismic gravity changes could be isolated only by carefully removing hydrological signals. **Citation:** Heki, K., and K. Matsuo (2010), Coseismic gravity changes of the 2010 earthquake in central Chile from satellite gravimetry, *Geophys. Res. Lett.*, *37*, L24306, doi:10.1029/2010GL045335.

1. Introduction

[2] Changes in the Earth's gravity field associated with earthquakes have been formulated nearly two decades ago [e.g., *Okubo*, 1991; *Sun and Okubo*, 1993]. The first reliable detection was made by an array of superconducting gravimeters after the 2003 Tokachi-Oki earthquake (M_w = 8.0), Japan [*Imanishi et al.*, 2004]. The two-dimensional distribution of coseismic gravity changes has been recovered for the first time by the GRACE satellites, launched in 2002 to investigate the time-variable gravity field, after the great Sumatra-Andaman (SA) earthquake (M_w = 9.1), 2004 December 26 [*Han et al.*, 2006].

[3] Fault dislocations modify the gravity fields by two mechanisms, i.e., deformation of layer boundaries with density contrasts (e.g., surface uplift and subsidence), and density changes of rocks due to volumetric strain (coseismic dilatation and compression). For an interplate thrust earthquake, uplift dominates vertical crustal movement, causing gravity increase localized around the epicentral area. Dilatation at the upper side of the down-dip end of the fault, on the other hand, causes gravity decrease of a longer wavelength [*Han et al.*, 2006]. The balance of these two principal factors is controlled, e.g., by thrust angles and fault depths; the latter (decrease) tends to be emphasized as the angle gets higher and the fault gets deeper.
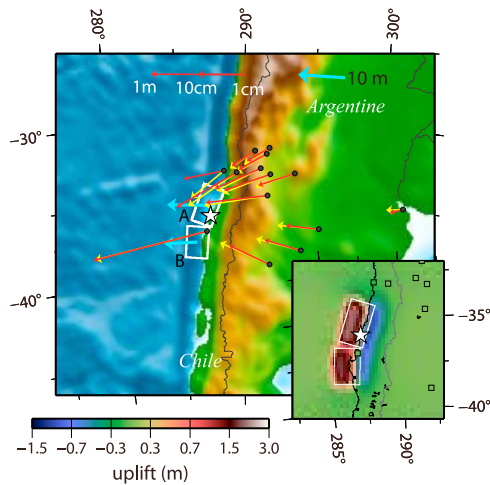
[4] No earthquakes since the 2004 SA event have left gravity signatures detectable with GRACE. It is likely that the 2005 Nias earthquake (M_w = 8.7), Indonesia, showed detectable coseismic gravity changes, but it was difficult to isolate those signals due to its spatial and temporal proximity to the 2004 SA event that occurred only 3 months earlier [*Einarsson et al.*, 2010]. The 2010 February 27 Chile earthquake (the Maule earthquake) (M_w = 8.8) ruptured the boundary between the Nazca and the South American Plates known as the Constitución-Concepción seismic gap [*Madariaga et al.*, 2010] (Figure 1). This is the largest earthquake after the 2004 SA earthquake, and has a good chance of showing coseismic gravity changes detectable with GRACE.

2. Observed Gravity Changes

[5] The Earth's gravity field is modeled as a superposition of spherical harmonics. A monthly GRACE data set consists of the coefficients of spherical harmonics (Stokes' coefficients) with degree and order complete to 60. Figure 2 shows the time series of monthly gravity values at (36S, 70W), ~250 km east of the epicenter, from 95 data sets (Level-2, RL04, Center for Space Research, Univ. Texas) spanning the period from 2002 April to 2010 May. We replaced the Earth's oblateness values (C_{20}) with those from Satellite Laser Ranging [*Cheng and Tapley*, 2004], and applied a fan filter with averaging radius of 300 km to reduce short wavelength noise [*Zhang et al.*, 2009]. We also reduced longitudinal stripes following *Swenson and Wahr* [2006], by using polynomials of degree 3 for coefficients with orders 15 or higher.

[6] In order to correct for changes in soil moisture, snow and canopy water, we used the Global Land Data Assimilation System (GLDAS) hydrological model [*Rodell et al.*, 2004]. After expanding equivalent water depth data in GLDAS/Noah to spherical harmonics, we applied the same fan filter (but not the de-striping filter) and converted them to gravity using equation (8) of *Wahr et al.* [1998]. They show seasonal changes with maxima in austral winter, and peak-to-peak amplitudes of ~5 μgal. After subtracting the GLDAS hydrological signal from GRACE data, we still find non-negligible amount of seasonal changes, caused by factors not adequately modeled in GLDAS, e.g., ground water. Here we modeled the corrected data after 2006.5 (relatively large inter-annual changes exist in data before 2006.5) with seasonal (annual and semiannual) and linear changes, together with coseismic jumps (Figure 2). We estimated such jumps with a grid point spacing of 0.2°, and drew their distribution in Figure 3a. The change is

[1]Department of Natural History Sciences, Hokkaido University, Sapporo, Japan.

Figure 1. Epicenter of the 2010 Chile earthquake after USGS (white star), and the two fault planes we assumed (white rectangles marked as A and B). Fault slips are shown by light blue arrows. The predicted and observed horizontal displacements of GPS stations (13 points from auxiliary Table 1 of *Delouis et al.* [2010] and an additional point, La Plata, "lpgs" from http://sopac.ucsd.edu) are shown by yellow and red arrows, respectively. Displacement arrow lengths are drawn proportionally to the common logarithm of the displacements (the length becomes zero for 1 cm displacement, see legend). Inset shows predicted coseismic vertical crustal movements (red: uplift, blue: subsidence, color scheme shown left). Squares in the inset show GPS stations, and are pasted with colors indicating observed uplifts with the same color scheme (colors are not conspicuous in the figure because even the largest observed vertical movement was 14 cm subsidence at Valparaiso).
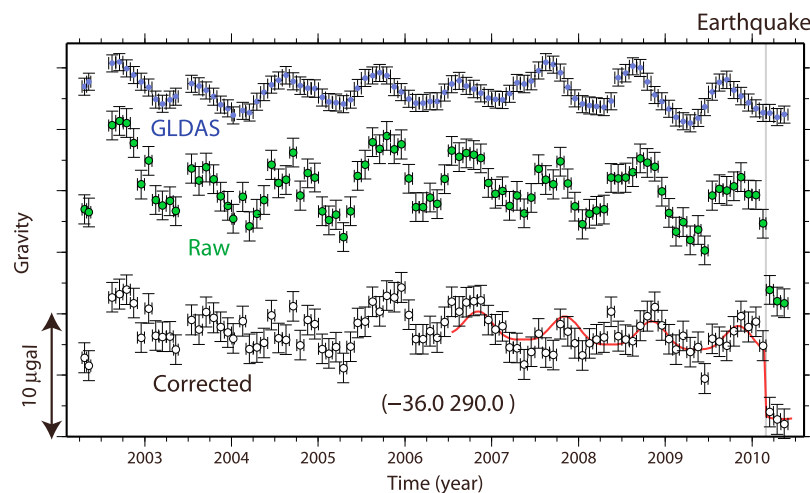
mostly negative, with the largest decrease of ~5 μgal located 200–300 km landward from the focal region. One-sigma formal errors of the jumps were typically ~1 μgal or less. This is the first clear example of coseismic

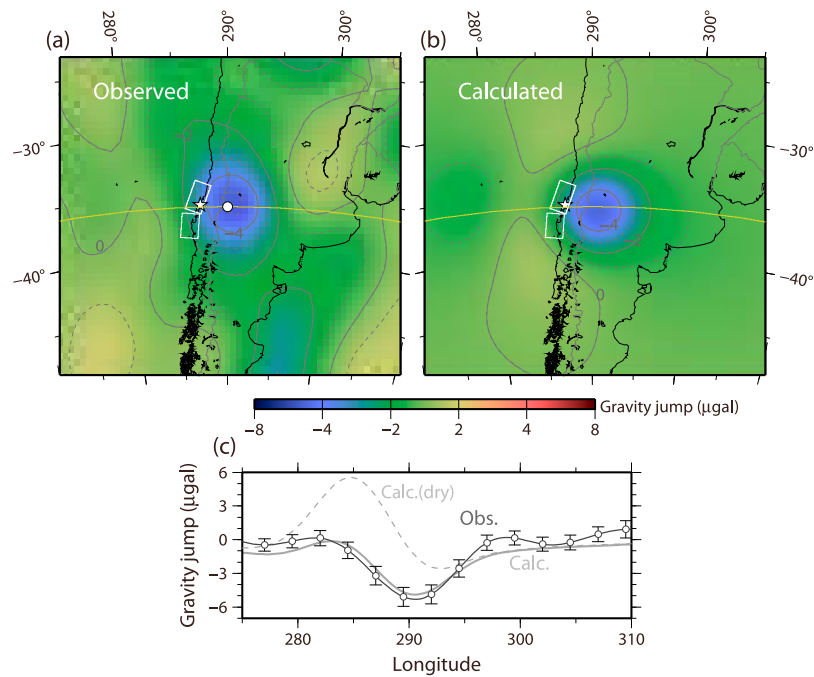gravity changes imaged with GRACE for earthquake with M_{w} less than nine.

3. Calculated Gravity Changes

[7] *Delouis et al.* [2010] reported fault parameters of the 2010 Chile earthquake inferred from coseismic displacements of GPS stations (red arrows in Figure 1) and Interferometric Synthetic Aperture Radar (InSAR) images. To calculate coseismic gravity changes, we assume a simpler model composed of two fault planes covering the two major asperities to the north (fault A, 270 km long) and south (fault B, 220 km long) of the epicenter. The faults were aligned with the trench (strikes 21°/6° for A/B), and the dips were fixed to 16° after *Ruegg et al.* [2009]. Interseismic crustal movements suggested locking depth down to 55 km [*Ruegg et al.*, 2009], but we assumed the depth 1–45 km for coseismic slips considering slip distribution results of *Delouis et al.* [2010]. Directions and amounts of slips were tuned so that the calculated displacements of the 14 continuous GPS stations agree with the observations (N88W/8.6 m, and N91W/7.0 m for faults A and B, respectively).

[8] Elastic half space assumption is inappropriate for points with focal distances larger than a few hundreds of kilometers. Hence we used the displacement Green's function for the stratified spherical Earth by *Sun et al.* [2009]. Calculated displacements (horizontal components shown by yellow arrows in Figure 1, and uplifts shown in its inset) generally show good agreement with the observations. Direction of the observed coseismic displacement of Valparaiso (northernmost coastal point) deviates by ~30° from the calculation. A more sophisticated fault model needs to be estimated by reoccupying near-field campaign GPS points densely deployed there [*Ruegg et al.*, 2009]. Uplift and subsidence are distributed mainly in the ocean and in land areas, respectively (Figure 1 inset). The inferred fault slip azimuths deviate clockwise by ~10° from the convergence direction of the Nazca and South American Plates by NUVEL-1 [*DeMets et al.*, 1990].

Figure 2. Time series of the monthly gravity values at 36S, 70W (white circle in Figure 3a) recovered by GRACE. A fan filter [*Zhang et al.*, 2009] and a de-striping filter [*Swenson and Wahr*, 2006] have been applied. Hydrological contributions (GLDAS/Noah, also fan-filtered) have been subtracted in the "corrected" time series. Corrected data after 2006.5 are modeled (red curve) by seasonal and linear changes with a coseismic jump. Error bars show one-sigma formal errors (assumed uniform) inferred a-posteriori to make the χ^2 of the post-fit residual unity.

Figure 3. (a) Geographical distribution of coseismic gravity jumps observed by GRACE, (b) calculated with the two fault model using *Sun et al.* [2009]. The GRACE observation has been corrected for GLDAS land hydrology. The same fan filter as GRACE has been applied to the calculated changes. Solid contours show −4, −2, and 0 μgal while broken contours show −3, −1, +1 μgal. (c) Comparison of profiles along latitude 36S, shown by yellow curves in Figures 3a and 3b. The broken curve shows the gravity change profile calculated without the sea water correction (see text). For the observed profile, one-sigma formal errors are shown every 2.5°.

[9] We used *Sun et al.*'s [2009] method to calculate gravity changes caused by the slips of faults A and B in a spherical earth. Because the original program assumed dry earth (i.e., surface uplift anywhere is interpreted as the replacement of air with crustal rock), we modified it so that a smaller density contrast (between crustal rock and sea water) is assumed for the vertical deformation of the sea floor. Calculated gravity changes after applying the 300 km fan filter (Figure 3b) is quite similar to those observed by GRACE (Figure 3a). Their profiles along the latitude −36° coincide with each other within observational uncertainties (Figure 3c). The sea water correction is important; the original gravity change profile had both positive and negative changes with comparable powers (dashed curve in Figure 3c), but the negative change dominates after the correction. As seen in Figure 1 inset, the uplifted region mainly resides under the sea, and gravity increase would have been reduced selectively by this correction.

4. Discussions

[10] Figure 3 shows consistent patterns and amplitudes of the observed and calculated gravity changes. This case, together with the 2004 SA earthquake case, improves our understanding of the mechanisms giving rise to coseismic gravity changes. The changes in the degree-2 tesseral components of the gravity (C_{21} and S_{21}) excite polar motion [e.g., *Chen and Wilson*, 2008]. The calculated coseismic gravity changes (Figure 3b) predict the pole shift of 2.8 milli-arc-seconds (mas) (~8.7 cm at the Earth's surface) toward 109.8E, which is close to the value cal-culated by R. Gross (e.g., *New Scientist*, March 2, 2010) as 2.7 mas.

[11] The 2004 SA earthquake showed distinct postseismic gravity changes (with a time constant of ~0.6 year) characterized by slow increase above the focal area. Past interpretations include the flow of supercritical water around the down-dip end of the fault [*Ogawa and Heki*, 2007], Burgers rheology of the low viscosity material in shallow mantle [*Panet et al.*, 2007, 2010; *Han et al.*, 2008], and afterslip in the down-dip and up-dip extension of the main rupture (T. Hasegawa et al., Rapid updip and slow downdip afterslips following the 2004 Sumatra-Andaman earthquake detected by GRACE, submitted to *Geophysical Journal International*, 2010). Postseismic crustal deformations have been observed with GPS numerous times. In contrast, postseismic gravity changes have been observed just once for the 2004 SA event, and its mechanism has not been well understood. We still have only a few months of GRACE data after the earthquake, too short to separate postseismic and hydrological gravity changes. It is important and interesting to keep investigating slow gravity changes in Central Chile over a long term.

References

Chen, J. L., and C. R. Wilson (2008), Low degree gravity changes from GRACE, Earth rotation, geophysical models, and satellite laser ranging, *J. Geophys. Res.*, *113*, B06402, doi:10.1029/2007JB005397.

Cheng, M., and B. D. Tapley (2004), Variations in the Earth's oblateness during the past 28 years, *J. Geophys. Res.*, *109*, B09402, doi:10.1029/2004JB003028.

Delouis, B., J.-M. Nocquet, and M. Vallée (2010), Slip distribution of the February 27, 2010 Mw = 8.8 Maule earthquake (central Chile) from static and high-rate GPS, InSAR, and broadband teleseismic data, *Geophys. Res. Lett.*, *37*, L17305, doi:10.1029/2010GL043899.

DeMets, C., R. G. Gordon, D. F. Argus, and S. Stein (1990), Current plate motions, *Geophys. J. Int.*, *101*, 425–478, doi:10.1111/j.1365-246X.1990.tb06579.x.

Einarsson, I., A. Hoechner, R. Wang, and J. Kusche (2010), Gravity changes due to the Sumatra-Andaman and Nias earthquakes as detected by the GRACE satellites: A reexamination, *Geophys. J. Int.*, *183*, 733–747, doi:10.1111/j.1365-246X.2010.04756.x.

Han, S.-C., C. K. Shum, M. Bevis, C. Ji, and C.-Y. Kuo (2006), Crustal dilatation observed by GRACE after the 2004 Sumatra-Andaman earthquake, *Science*, *313*, 658–662, doi:10.1126/science.1128661.

Han, S.-C., J. Sauber, S. Luthcke, C. Ji, and F. Pollitz (2008), Postseismic gravity change following the great 2004 Sumatra-Andaman earthquake from the regional harmonic analysis of GRACE inter-satellite tracking data: Implication for the regional viscoelastic response, *J. Geophys. Res.*, *113*, B11413, doi:10.1029/2008JB005705.

Imanishi, Y., T. Sato, T. Higashi, W. Sun, and S. Okubo (2004), A network of superconducting gravimeters detects submicrogal coseismic gravity changes, *Science*, *306*, 476–478, doi:10.1126/science.1101875.

Madariaga, R., M. Métois, C. Vigny, and J. Campos (2010), Central Chile finally breaks, *Science*, *328*, 181–182, doi:10.1126/science.1189197.

Ogawa, R., and K. Heki (2007), Slow postseismic recovery of geoid depression formed by the 2004 Sumatra-Andaman earthquake by mantle water diffusion, *Geophys. Res. Lett.*, *34*, L06313, doi:10.1029/2007GL029340.

Okubo, S. (1991), Potential and gravity changes raised by point dislocations, *Geophys. J. Int.*, *105*, 573–586, doi:10.1111/j.1365-246X.1991.tb00797.x.

Panet, I., et al. (2007), Coseismic and post-seismic signatures of the Sumatra 2004 December and 2005 March earthquakes in GRACE satellite gravity, *Geophys. J. Int.*, *171*, 177–190, doi:10.1111/j.1365-246X.2007.03525.x.

Panet, I., F. Pollitz, V. Mikhailov, M. Diament, P. Banergee, and K. Grijalva (2010), Upper mantle rheology from GRACE and GPS postseismic deformation after the 2004 Sumatra-Andaman earthquake, *Geochem. Geophys. Geosyst.*, *11*, Q06008, doi:10.1029/2009GC002905.

Rodell, M., et al. (2004), The Global Land Data Assimilation System, *Bull. Am. Meteorol. Soc.*, *85*, 381–394, doi:10.1175/BAMS-85-3-381.

Ruegg, J. C., A. Rudloff, C. Vigny, R. Madariaga, J. B. de Chaballer, J. Campos, E. Kausel, S. Barrientos, and D. Dimitrov (2009), Interseismic strain accumulation measured by GPS in the seismic gap between Constitución and Concepción in Chile, *Phys. Earth Planet. Inter.*, *175*, 78–85, doi:10.1016/j.pepi.2008.02.015.

Sun, W., and S. Okubo (1993), Surface potential and gravity changes due to internal dislocations in a spherical Earth—1. Theory for a point dislocation, *Geophys. J. Int.*, *114*, 569–592, doi:10.1111/j.1365-246X.1993.tb06988.x.

Sun, W., S. Okubo, G. Fu, and A. Araya (2009), General formulations of global and co-seismic deformations caused by an arbitrary dislocation in a spherically symmetric earth model—Applicable to deformed earth surface and space-fixed point, *Geophys. J. Int.*, *177*, 817–833, doi:10.1111/j.1365-246X.2009.04113.x.

Swenson, S. C., and J. Wahr (2006), Post-processing removal of correlated errors in GRACE data, *Geophys. Res. Lett.*, *33*, L08402, doi:10.1029/2005GL025285.

Wahr, J., M. Molenaar, and F. Bryan (1998), Time variability of the Earth's gravity field: Hydrological and oceanic effects and their possible detection using GRACE, *J. Geophys. Res.*, *103*, 30,205–30,229, doi:10.1029/98JB02844.

Zhang, Z. Z., B. F. Chao, Y. Lu, and H. T. Hsu (2009), An effective filtering for GRACE time-variable gravity: Fan filter, *Geophys. Res. Lett.*, *36*, L17311, doi:10.1029/2009GL039459.

K. Heki and K. Matsuo, Department of Natural History Sciences, Hokkaido University, N10 W8, Kita-ku, Sapporo, Hokkaido 060-0810, Japan. (heki@mail.sci.hokudai.ac.jp)